Draft version December 17, 2018
Typeset using LaTeX default style in AASTeX62

Deep Hyper Suprime-Cam Images and a Forced Photometry Catalog in W-CDF-S

Q. Ni,[1] J. Timlin,[1] W. N. Brandt,[1] and G. Yang[1]

[1] *Department of Astronomy & Astrophysics, 525 Davey Lab, The Pennsylvania State University, University Park, PA 16802, USA*

ABSTRACT

The Wide Chandra Deep Field-South (W-CDF-S) field is one of the SERVS fields with extensive multiwavelength datasets, which can provide insights into the nature and properties of objects in this field. However, the public optical data from DES (*grizy* to $m_{\rm AB} \approx 21.4 - 24.3$) are not sufficiently deep to match well the NIR data from VIDEO ($ZYJHK_s$ to $m_{\rm AB} \approx 23.5 - 25.7$), which limits the investigation of fainter objects at higher redshifts. Here, we present an optical catalog of $\approx$ 2,000,000 objects in W-CDF-S utilizing archival Hyper Suprime-Cam observations in the *g,r,i,z* bands covering ≈ 5.7 deg^2. The estimated depth is ≈ 25.9 for *g*-band, 25.6 for *r*-band, 25.8 for *i*-band, and 25.2 for *z*-band, which is deep enough to complement the NIR data, and will benefit AGN/galaxy studies in W-CDF-S in the future.

Keywords: catalogs — surveys — galaxies: general — galaxies: active

The Wide Chandra Deep Field-South (W-CDF-S) region is a ≈ 4.5 deg^2 field in the SERVS (Mauduit et al. 2012) CDF-S footprint. W-CDF-S has extensive multiwavelength coverage that is publicly available, such as ATLAS (Franzen et al. 2015) in the radio, HerMES (Oliver et al. 2012) in the FIR, SERVS and VIDEO (Jarvis et al. 2013) in the NIR, and DES (Abbott et al. 2018) in the optical. PRIMUS (Coil et al. 2011) also provides more than 30,000 spectroscopic redshifts in the field (see Table 1 of Chen et al. 2018 for more details). Furthermore, W-CDF-S will have ≈ 2.2 Ms of *XMM-Newton* coverage by 2020 covering the whole field, in addition to the archival X-ray coverage in the ≈ 0.3 deg^2 CDF-S (Comastri et al. 2016; Xue et al. 2016; Luo et al. 2017). However, the current public optical data from DES (*grizy* to $m_{\rm AB} \approx 21.4 - 24.3$) do not delve as deep as the NIR data from VIDEO ($ZYJHK_s$ to $m_{\rm AB} \approx 23.5 - 25.7$). Thus, optical data at least as deep as the NIR data will benefit the investigation of fainter objects at higher redshifts.

Here, we present an optical catalog of archival Hyper Suprime-Cam (HSC; Miyazaki et al. 2012) observations in W-CDF-S. HSC is an optical digital camera attached to the Subaru Telescope. We obtained the publicly available raw image data in the *g,r,i,z* bands (taken between January 2015 and March 2017) and relevant calibration files via SMOKA.[1] The coverage of HSC is shown in Figure 1 along with some other key multiwavelength data in the W-CDF-S region. Observations in the *g,i,z* bands cover the full ≈ 5.7 deg^2 area shown in Figure 1, while observations in the *r*-band only cover the central ≈ 2.0 deg^2 region. These observations have exposure times close to the Deep fields in the HSC Subaru Strategic Program (Aihara et al. 2018).

We analyzed the HSC data with `hscPipe` v5.4 (Bosch et al. 2018), a version of the LSST Software Stack (Ivezić et al. 2008; Axelrod et al. 2010; Jurić et al. 2017), following the `hscPipe` user manual.[2] The pipeline first performs single-visit processing, which includes the subtraction of overscan, bias, and dark, and also flatfielding. Then, it calibrates the relative position and flux scale of each CCD against the PanSTARRS1 (PS1) PV3 catalog (Magnier et al. 2013). Utilizing the corrected position and flux scale, CCD images are warped and combined using a weighted average to reduce contamination. Sources are then detected and measured in the *g,r,i,z* bands separately, and a list of sources is generated by merging the object information from all the bands. Finally, forced photometry is performed in the four bands simultaneously with source positions and shape parameters fixed to the values of a well-detected reference band selected by `hscPipe` (see Bosch et al. 2018 for details).

Corresponding author: Qingling Ni, John Timlin
qxn1@psu.edu, jxt811@psu.edu

[1] https://smoka.nao.ac.jp
[2] https://hsc.mtk.nao.ac.jp/pipedoc_5_e/

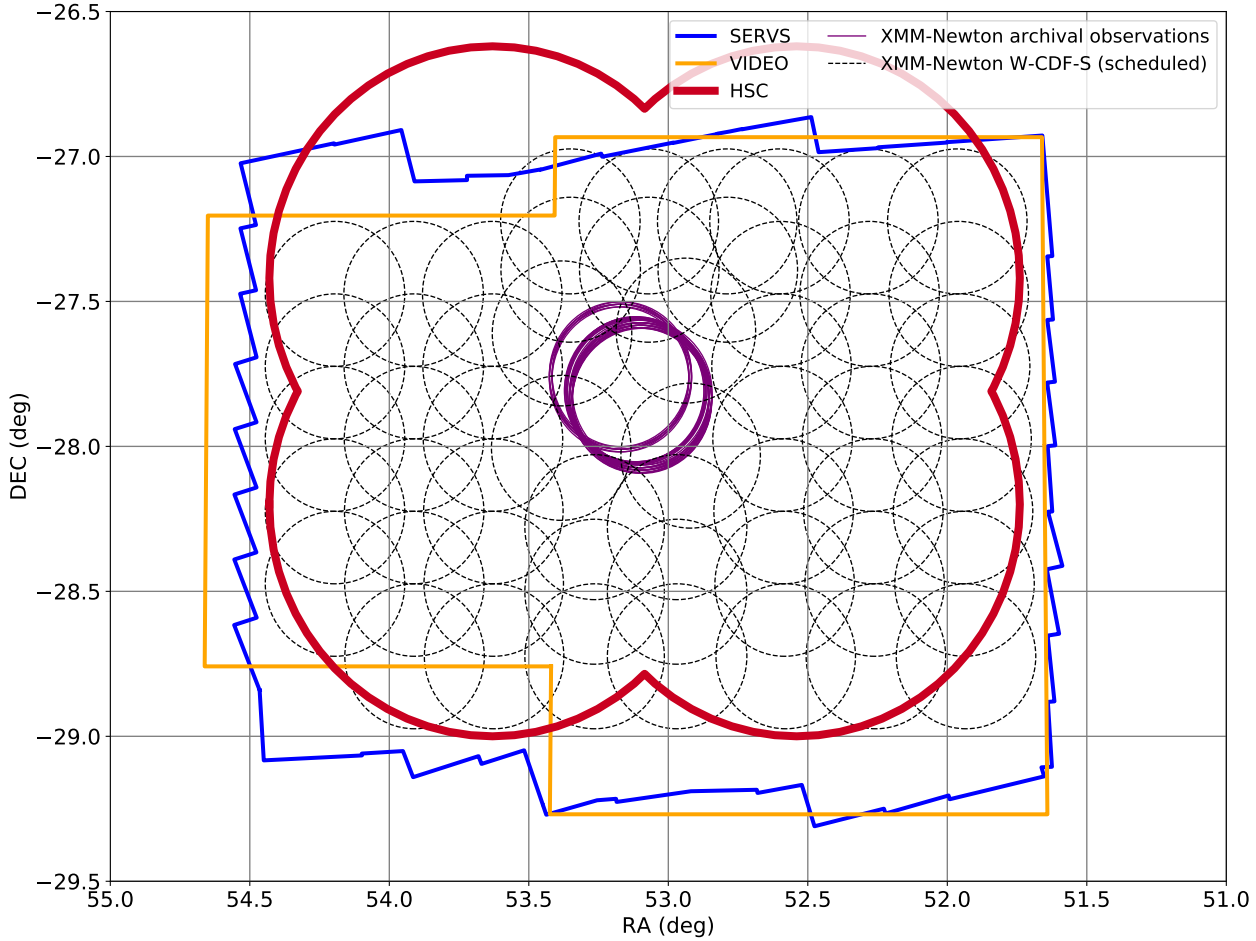

Figure 1. The multiwavelength coverage of the W-CDF-S field shown as labelled.

We present the coadded images and the forced photometry catalog at 10.5281/zenodo.2225161. Corresponding weight maps and mask images are also provided, which contain information about the coadded image quality pixel by pixel. To use the catalog products, users should use the suggested flag cuts (e.g., Table 4 of Aihara et al. 2018) to select objects with clean photometry. We also created a `flag_clean` column to mark "clean" objects (the selection criteria are shown in the catalog schema).

We also provide a few diagnostic plots to demonstrate the astrometric and photometric quality of the catalog in the Appendix. In Figure S1, we show the number of sources as a function of the PSF magnitude in each band for "clean" objects. The estimated depth is ≈ 25.9 for g-band, 25.6 for r-band, 25.8 for i-band, and 25.2 for z-band. The depths as a function of the patch location are shown in Figure S2. Also, HSC-to-*Gaia* (Gaia Collaboration 2018) positional offsets are presented in Figure S3, demonstrating the astrometric quality of the HSC data products. Other diagnostic plots are also available.

Finally, we provide a preliminary match of the HSC sources to their infrared counterparts. We matched the "clean" HSC objects as well as detections in VIDEO to the SERVS source positions within $1''$ to generate an optical-IR catalog of sources in W-CDF-S.

We note that the VOICE Survey (Vaccari et al. 2016) data will be released in the near future, which has u, g, r, i bands down to $m_{\rm AB} \approx 25-26$ for a somewhat different 4 deg^2 footprint. Also, the "Cosmic Dawn Survey" will provide deeper *Spitzer* (PI: P. Capak) and HSC (PIs: D. Sanders & P. Capak) coverage in W-CDF-S in the coming years.

We thank the anonymous PI of the HSC data products we used in W-CDF-S. We thank Yoshihiko Yamada at the `hscPipe` help desk, for assistance with `hscPipe`. We thank Ian Smail and Michael Strauss for helpful discussions.

REFERENCES

Abbott, T. M. C., Abdalla, F. B., Allam, S., et al. 2018, arXiv:1801.03181.

Aihara, H., Armstrong, R., Bickerton, S., et al. 2018, PASJ, 70, S8

Axelrod, T., Kantor, J., Lupton, R. H., & Pierfederici, F. 2010, Proc. SPIE, 7740, 774015

Bosch, J., Armstrong, R., Bickerton, S., et al. 2018, PASJ, 70, S5

Chen, C.-T. J., Brandt, W. N., Luo, B., et al. 2018, MNRAS, 478, 2132.

Coil, A. L., Blanton, M. R., Burles, S. M., et al. 2011, ApJ, 741, 8.

Comastri, A., Iwasawa, K., Vignali, C., et al. 2016, arXiv:1612.00955

Franzen, T. M. O., Banfield, J. K., Hales, C. A., et al. 2015, MNRAS, 453, 4020.

Gaia Collaboration, 2018, A&A, 616, A1

Ivezić, Ž., Kahn, S. M., Tyson, J. A., et al. 2008, arXiv:0805.2366

Jarvis, M. J., Bonfield, D. G., Bruce, V. A., et al. 2013, MNRAS, 428, 1281.

Jurić, M., Kantor, J., Lim, K.-T., et al. 2017, Astronomical Data Analysis Software and Systems XXV, 512, 279

Luo, B., Brandt, W. N., Xue, Y. Q., et al. 2017, ApJS, 228, 2

Magnier, E. A., Schlafly, E., Finkbeiner, D., et al. 2013, ApJS, 205, 20

Mauduit, J.-C., Lacy, M., Farrah, D., et al. 2012, Publications of the Astronomical Society of the Pacific, 124, 714.

Miyazaki, S., Komiyama, Y., Nakaya, H., et al. 2012, Proc. SPIE, 8446, 84460Z

Oliver, S. J., Bock, J., Altieri, B., et al. 2012, MNRAS, 424, 1614.

Vaccari, M., Covone, G., Radovich, M., et al. 2016, Proceedings of the 4th Annual Conference on High Energy Astrophysics in Southern Africa (HEASA 2016). 25-26 August, 26.

Xue, Y. Q., Luo, B., Brandt, W. N., et al. 2016, ApJS, 224, 15.

APPENDIX

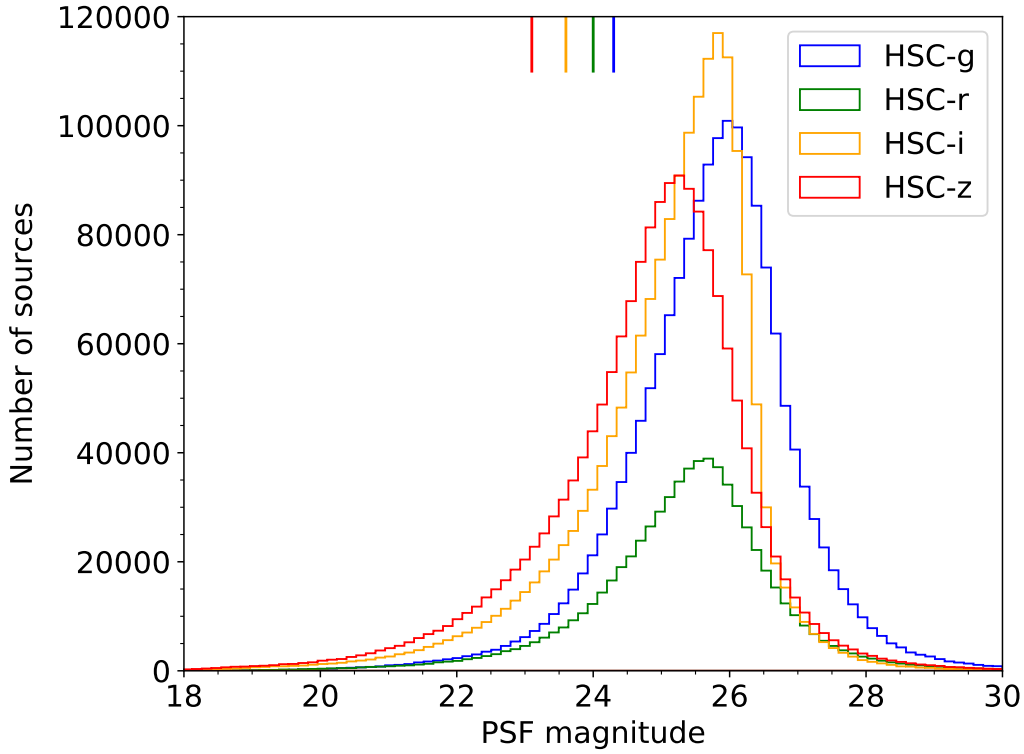

Figure S1. Histograms showing the distributions of PSF magnitudes for "clean" objects in the coadded HSC catalog. An estimation of the observation depth can be obtained by finding the mode of the magnitude distribution. The estimated depth is ≈ 25.9 for g-band, 25.6 for r-band, 25.8 for i-band, and 25.2 for z-band. For comparison, the depths of DES DR1 data in the g, r, i, z bands are plotted as vertical bars with the color blue, green, orange, and red.

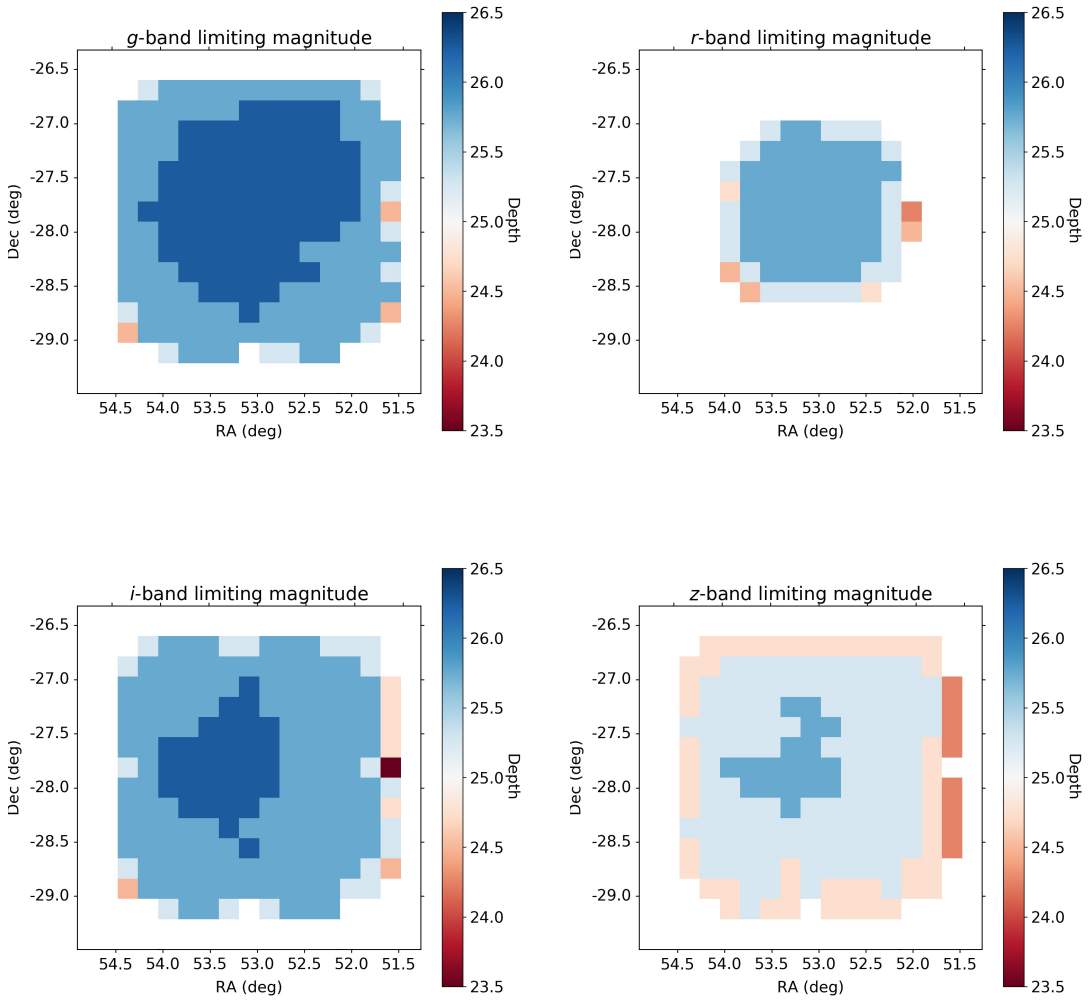

Figure S2. Patch-by-patch depth maps for the g, r, i, z bands. The depths here are estimated by the mode of the PSF magnitude distribution in each patch.

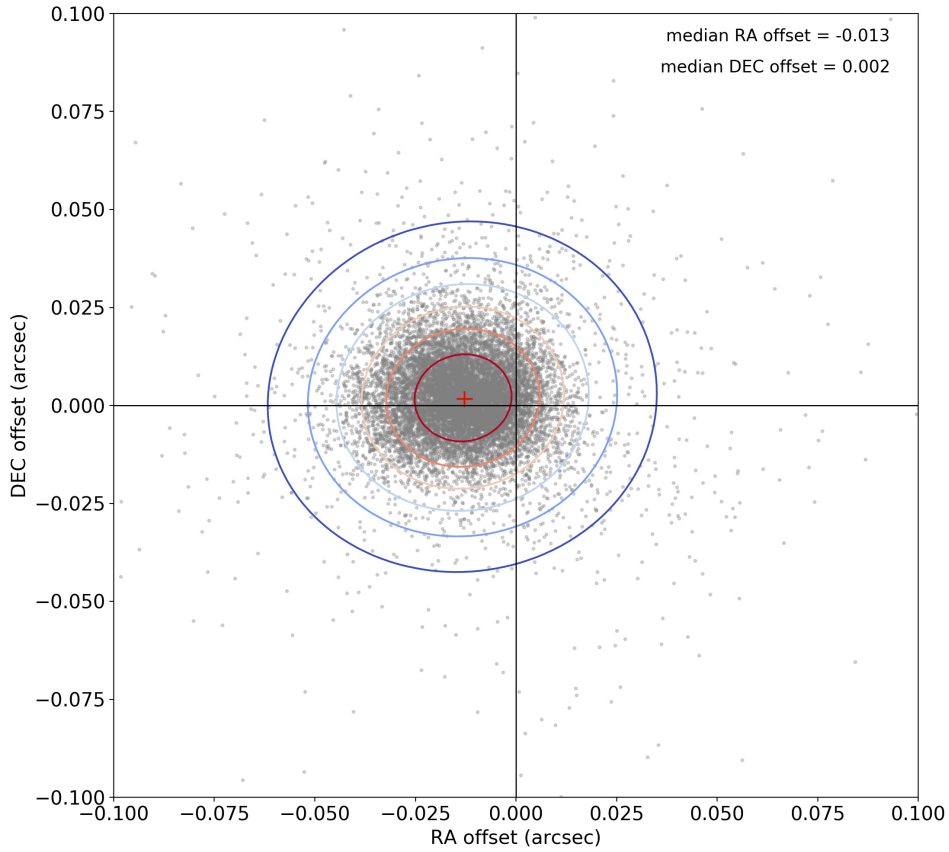

Figure S3. Distribution of the HSC-to-*Gaia* positional offsets in the RA versus Dec plane. The contours represent the isodensity levels of the points. The median positional offset is represented by the red cross. We give equations to correct to the *Gaia* astrometric frame in `readme.txt`.

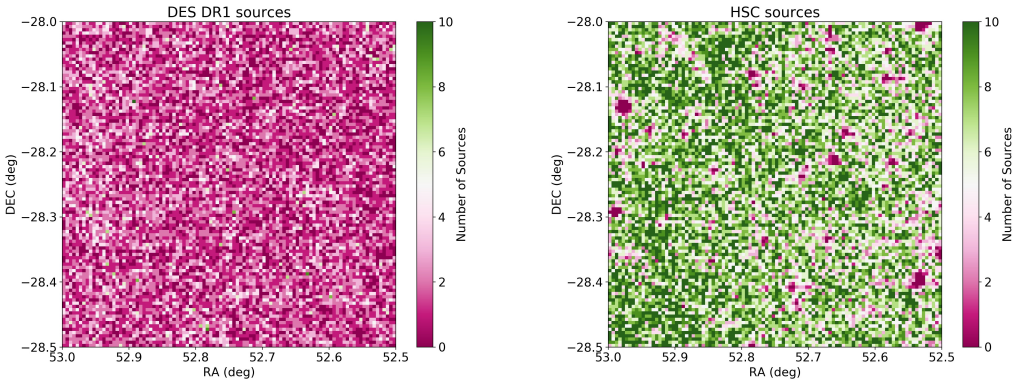

Figure S4. 2D histograms of the number of i-band detected sources in DES DR1 (left) and HSC (right) in the same 0.25 deg^2 region in W-CDF-S. Note that the two panels have the same color scale. The HSC observations increase the number density of optical sources by a factor of ≈ 10.

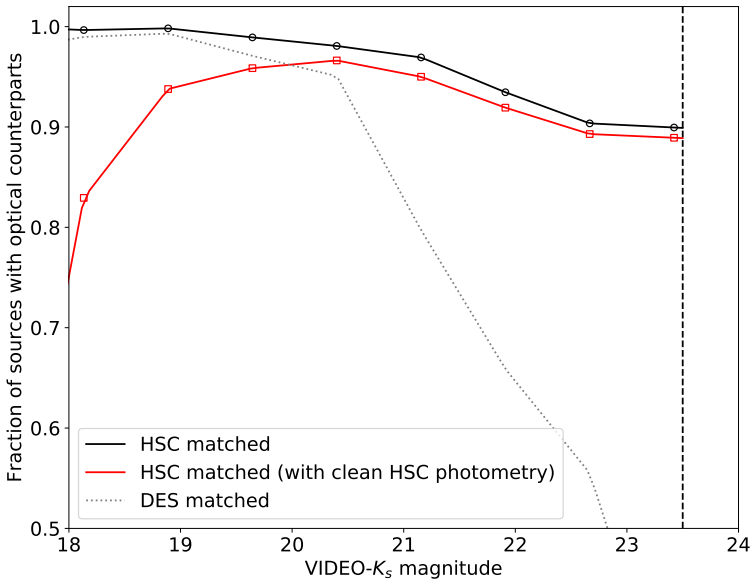

Figure S5. The fraction of VIDEO sources that have optical counterparts within 1" at the given VIDEO-K_s magnitude vs. the VIDEO-K_s magnitude. The black open circles and the black solid line represent the fraction of VIDEO sources with HSC counterparts at the given magnitude; the red open squares and the red solid line represent the fraction of VIDEO sources with "clean" HSC counterparts (`flag_clean == True`) at the given magnitude; the gray dotted line represents the fraction of VIDEO sources with DES counterparts at the given magnitude. The vertical black dashed line represents the limiting magnitude of the K_s-band reported in VIDEO. The HSC data are deep enough to match with VIDEO sources, while the DES data are not deep enough to match with VIDEO sources. The drop of the matched fraction with "clean" HSC objects at the bright end is a result of the low saturation level of HSC (for "clean" HSC objects, we require that the center of the source is not saturated).

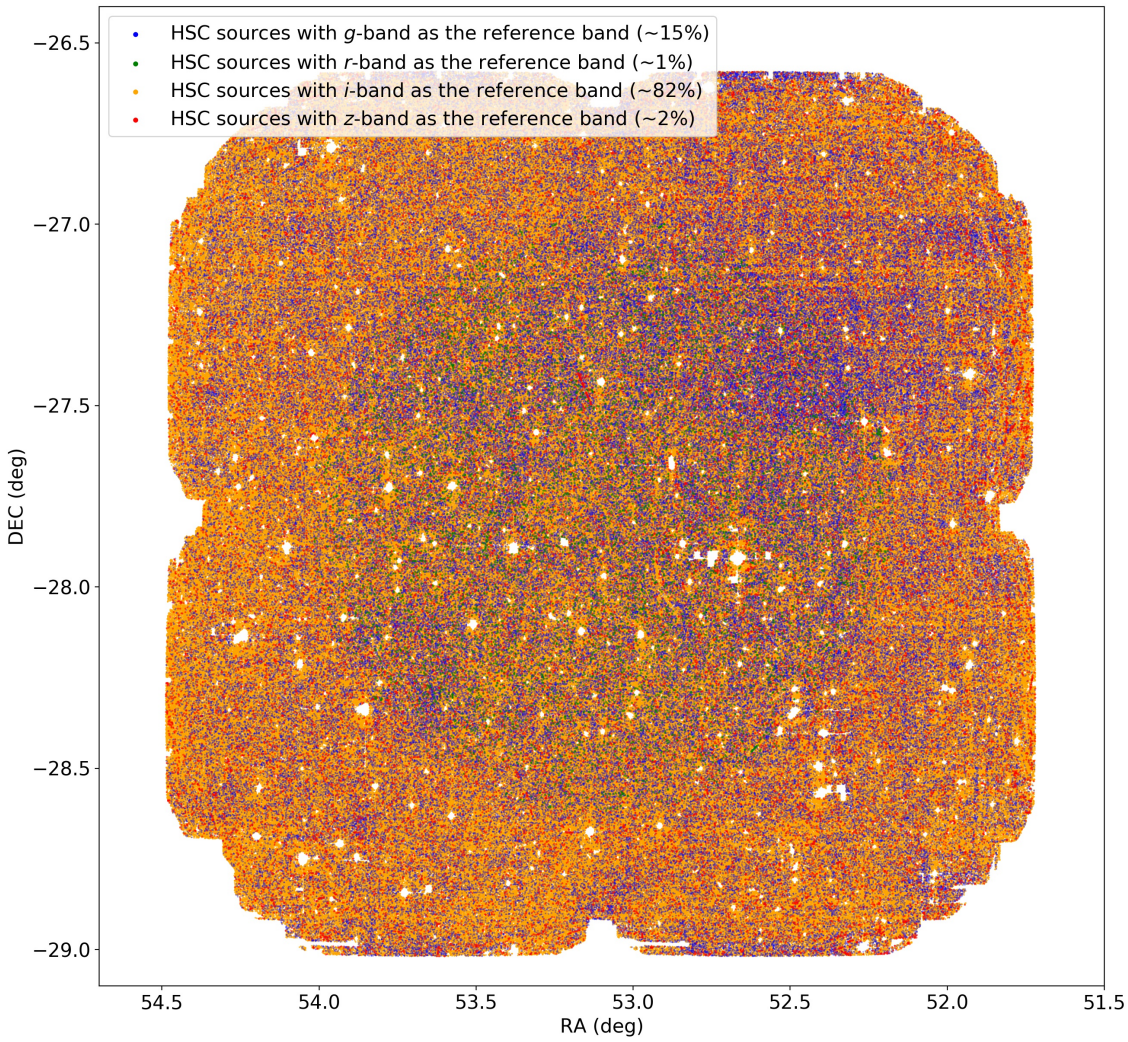

Figure S6. The map of "clean" objects in the forced-photometry catalog. Circles with different colors represent sources with different reference bands used when performing the forced photometry. Most of the sources have the i-band as the reference band.

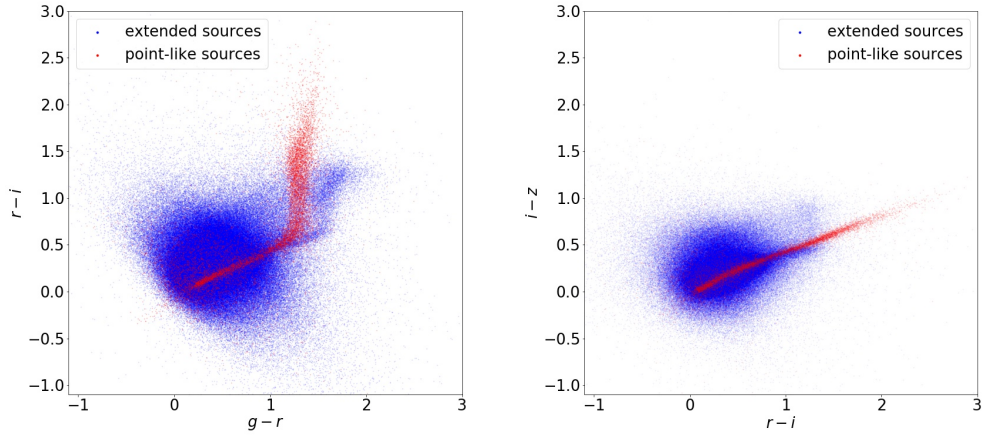

Figure S7. $g - r$ vs. $r - i$ (left) and $r - i$ vs. $i - z$ (right) plots for "clean" objects in the coadded HSC catalog with i-band magnitude < 25, and the magnitudes in the g, i, z bands being brighter than the estimated depth of that band (the magnitudes have not been corrected for Galactic extinction). The extended sources (represented by the blue dots) are selected by requiring `hsm_point_like == False`, and the point-like sources (represented by the red dots) are selected by requiring `hsm_point_like == True`.